Food Chemistry 134 (2012) 1959–1966

Contents lists available at SciVerse ScienceDirect

Food Chemistry

journal homepage: www.elsevier.com/locate/foodchem

Total flavan glycoside from *Abacopteris penangiana* rhizomes and its acid hydrolysate: Characterisation and anti-benign prostatic hyperplasia potential

Han Wei [a], Guanghua Wu [b], Du Shi [a], Shanshan Song [a], Xuenong Zhang [a], Yongfang Lei [b], Jinlan Ruan [a,*]

[a] Key Laboratory of Natural Medicinal Chemistry and Resource Evaluation, School of Pharmacy, Tongji Medical College, Huazhong University of Science and Technology, Wuhan, China
[b] Department of pharmacy, Tongji hospital, Tongji Medical College, Huazhong University of Science and Technology, Wuhan, China

ARTICLE INFO

Article history:
Received 15 January 2012
Received in revised form 21 March 2012
Accepted 28 March 2012
Available online 5 April 2012

Keywords:
Abacopteris penangiana
Benign prostatic hyperplasia
Dihydrotestosterone
Growth factor
Apoptosis

ABSTRACT

This study was conducted to characterise the flavonoid components of total flavan glycoside from *Abacopteris penangiana* rhizomes (TFA) and its acid hydrolysate (AHT) through HPLC–DAD–ESI–MS/MS analysis, and to investigate the hypothesis that TFA and AHT exhibit anti-benign prostatic hyperplasia (BPH) potential in castrated rats with testosterone-induced BPH. HPLC–MS/MS analysis indicated that TFA is rich in flavan-4-ol glycosides and AHT mainly contains 3-deoxygenated anthocyanidin. After 4 weeks of administration, TFA and AHT successfully decreased the prostate index and prostate specific antigen plasma concentrations in the rats. Histoarchitectural improvement in the prostate gland was also observed. Reduced dihydrotestosterone, VEGF, bFGF, EGF, and KGF levels were observed both in TFA- and AHT-treated rats. Furthermore, the prostatic expression of Blc-2 was inhibited, whereas that of Bax and p53 was activated by TFA and AHT. In conclusion, TFA and AHT have anti-BPH properties. Hence, plants with flavan glycosides have potential use in the treatment of BPH.

1. Introduction

The prostate is the secondary endocrine organ of males. Benign prostatic hyperplasia (BPH) is a progressive condition characterised by prostate enlargement, accompanied by lower urinary tract symptoms (Briganti et al., 2009). Considering the high incidence of BPH in humans (Napalkov, Maisonneuve, & Boyle, 1995) and the influence of this condition on the quality of life of patients, the treatment of this disease is a priority for public health. The aetiology of BPH is complicated and remains unclear to date; recent novel findings highlight the key role of aging, hormonal alterations, metabolic syndrome, and inflammation (Briganti et al., 2009; Thompson & Yang, 2009; Untergasser, Madersbacher, & Berger, 2005).

Abacopteris penangiana (Hook.) Ching (Thelypteridaceae) is a fern widely distributed throughout the south of China, India, and Nepal. For a long time now, the Tujia ethnic group has been using *A. penangiana* rhizome, *Jixuelian* in Chinese, as a folk herbal medicine to treat blood stasis, blood circulation barriers, oedema, and inflammation in patients suffering from metabolic syndrome. Furthermore, *A. penangiana* has been proven to contain many novel flavan-4-ol glycosides (Zhao, Jin, Ruan, Cai, & Zhu, 2008; Zhao, Ruan, Jin, Zhu, & Lin, 2010; Zhao, Ruan, Jin, Zhu, & Yu, 2011; Zhao et al., 2006; Zhao et al., 2007).

Presently, phytotherapeutics has become a popular method for the treatment of BPH. Studies have proven that many plants, including *Sphaeranthus indicus* (Nahata & Dixit, 2011), *Echinacea purpurea* (Skaudickas, Kondrotas, Kevelaitis, & Venskutonis, 2009), and *Roystonea regia* (Pérez et al., 2008), possess anti-BPH potential. As part of a bigger study that seeks to develop effective anti-BPH drugs from Chinese herbal medicines, the present research characterised the total flavan glycoside in *A. penangiana* rhizomes (TFA, Fig. 1-I), as well as the acid hydrolysate (AHT, Fig. 1-I) of the compound, through high performance liquid chromatography–diode array detector–electrospray ionisation–tandem mass spectrometry (HPLC–DAD–ESI–MS/MS) analysis, and investigated the anti-BPH potential of TFA and AHT in castrated rats with testosterone-induced prostatic hyperplasia.

2. Materials and methods

2.1. Plant material

Dried *A. penangiana* rhizomes were collected in June 2010 in Enshi County, Hubei, China, and authenticated by Prof. Ceming Tan of the Jiujiang Forest Plants Specimen Mansion. The voucher specimen (PZX0311) was deposited in School of Pharmacy, Tongji Medical College, Huazhong University of Science and Technology.

2.2. Sample preparation

TFA was prepared following a reported method (Wei, Ruan, Lei, & Yang, 2012). Powdered rhizomes (1 kg) were exhaustively extracted with 80% EtOH (3 × 6 L) under reflux, and then

* Corresponding author. Fax: +86 27 83692762.
E-mail addresses: weihan548@126.com, jinlan8152@163.com (J. Ruan).

0308-8146/$ - see front matter © 2012 Elsevier Ltd. All rights reserved.
http://dx.doi.org/10.1016/j.foodchem.2012.03.128

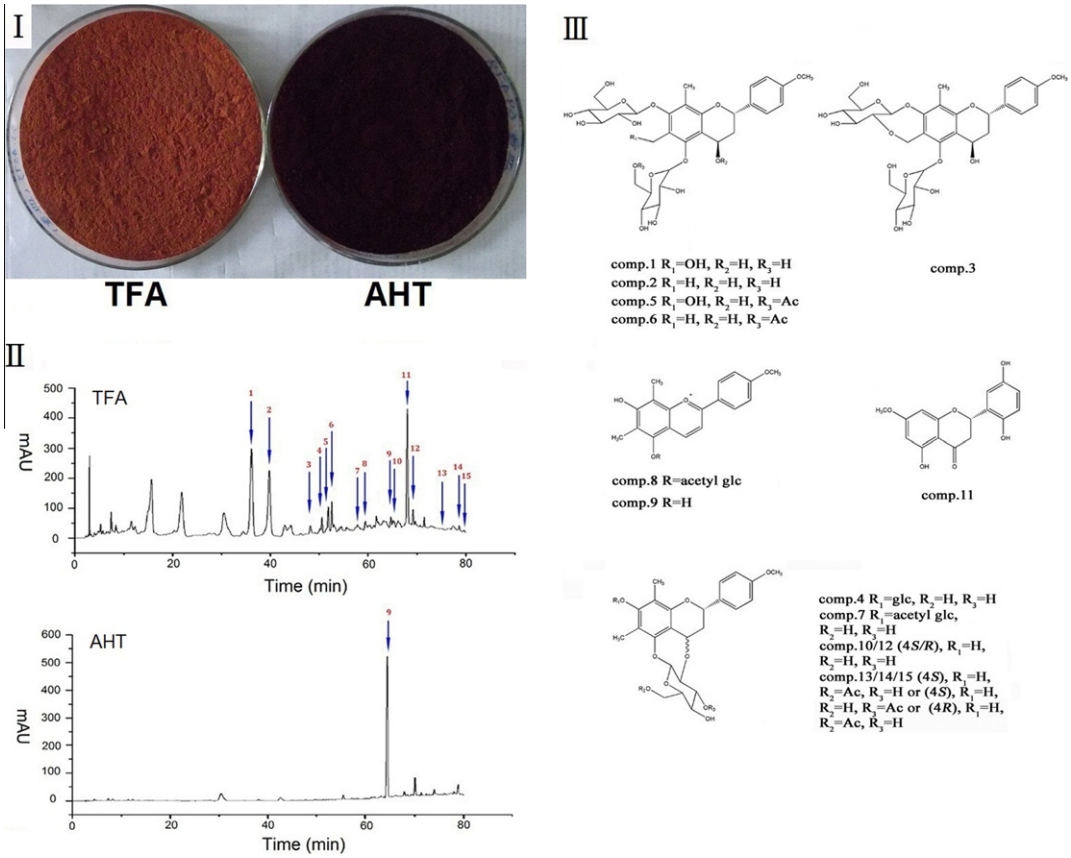

Fig. 1. (I) Photograph of TFA and AHT; (II) HPLC chromatogram of TFA and AHT; (III) the chemical structures of compounds 1–15.

concentrated to dryness under vacuum at 50 °C, to obtain crude extract (150 g). The extract was then dissolved in water (5 L), and the resulting solution was poured into a chromatography column (10 × 60 cm, porous polymer resins HPD500, Bonherb Technology Company, Hebei, China). The absorbed resins were initially eluted with water (35 L) to remove extraneous constituents with strong polarity, then with 70% EtOH (30 L) to increase the amount of flavan glycosides obtained. The evaporation of the 70% EtOH eluate under 50 °C yielded TFA (73.5 g).

AHT was prepared following a reported method (Zhao et al., 2006). Briefly, a solution of TFA (35.5 g) and 10% HCl (700 mL) was stirred at 95 °C for 6 h, and then at 45 °C overnight. The reaction mixture was cooled at 4 °C for 1 h, and then filtered to collect undissolved substances. AHT (25.9 g) was obtained after vacuum desiccation under 35 °C.

2.3. HPLC–DAD–ESI–MS/MS analysis

Analysis was performed using liquid chromatography (LC) interfaced with ion trap mass spectrometry. The LC system (Agilent 1100 Series, Agilent Technologies, Waldbronn, Germany) was equipped with a vacuum degasser, a binary pump, a column oven, an autosampler, and a photodiode-array detector (DAD). Chromatography was carried out in an amethyst C18-p column (Sepax-tech®, 4.6 mm × 20 mm, 5 μm) with the flow rate of the gradient elution at 1 mL/min. The analytical column was thermostated at 30 °C.

The initial composition of the mobile phase was 17% A and 83% B (A = acetonitrile; B = H_2O + 0.2% acetic acid). Samples were analysed with the following gradient: 17% A for 3 min, from 17% to 19% A in 22 min, from 19% to 21% A in 13 min, from 21% to 29% A in 13 min, from 29% to 30% A in 4 min, from 30% to 45% A in 20 min, and 45% A for 5 min. Samples were filtered using a 0.45-μm filter. Injection volume was 10 μL, and detection was carried out between 200 and 600 nm.

The LC/MSD Trap XCT ion trap mass spectrometer (Agilent) was equipped with an electrospray ion source with a nebuliser spacer. The operating conditions of the ESI interface in the positive-ion mode were as follows: drying gas (N_2) temperature, 325 °C; drying gas flow 10 L/min; nebuliser gas (N_2) pressure, 40 psi; and capillary voltage, 3500 V. The trapping parameters were set to a maximum accumulation time of 200 ms at an *m/z* range of *m/z* 100 to *m/z* 1000. A narrow isolation width of *m/z* 0.2 was selected. System control and data analysis were performed by Agilent LC ChemStation and Bruker Daltonics Trap Control and QuantAnalysis, respectively.

2.4. Animal experiments for anti-BPH potential

2.4.1. Animals

A total of 84 adult male Sprague–Dawley rats weighing 170 ± 20 g were acquired from the Animal Center of the Tongji Medical Center of Huazhong University of Science and Technology (Wuhan, China). The animals were housed under controlled conditions (temperature 25 ± 2 °C; relative humidity 65 ± 5%; and 12-h light/dark cycles) and were allowed free access to water and food pellets for 1 week before and during the experiments. All experiments were performed in compliance with the Chinese legislation on the use and care of laboratory animals and were approved by the Committee on Animal Care and Use of the Huazhong University of Science and Technology.

2.4.2. Animal treatments and experimental designs

BPH was induced in the rats by subcutaneous injection of testosterone after castration (Naslund & Coffey, 1986; Sun et al., 2008). Briefly, after anaesthetisation with chloral hydrate

(350 mg/kg body weight, i.p.), the scrota of 10 rats in the negative control group were cut open and then sewed up without cutting off the testicles; 74 other rats were castrated. After the surgical operation, four rats died because of narcotic overdose. The other 70 were randomly divided into 6 groups. The following treatments were administered through injection for 4 weeks: negative control group, corn oil (i.h.; $n = 10$); BPH model group, corn oil mixed with testosterone (i.h., 10 mg/kg per day; $n = 11$); positive control group, testosterone mixed with finasteride (i.g., 1 mg/kg per day; $n = 11$); TFA low/high dose group, testosterone mixed with TFA (i.g., 100 or 200 mg/kg per day, respectively; each group, $n = 12$); and AHT low/high dose group, testosterone mixed with AHT (i.g., 100 or 200 mg/kg per day, respectively; each group $n = 12$). The dosage of TFA and AHT was fixed based on the literature (Chen et al., 2011; Jang et al., 2010). During the experiment, no external morphological and behavioural changes were observed in the rats treated at these dose levels.

After the final treatment, the rats were deprived of food overnight, but were allowed free access to water. In the morning of the next day, animals were weighed and then sacrificed. Blood was collected and allowed to clot, and then the serum was separated at 3500 rpm for 15 min and stored at −80 °C until the assessment of prostate specific antigen (PSA) and dihydrotestosterone (DHT) plasma levels was performed. Prostates were rapidly excised, weighed, and sectioned. A section of each prostate was stored at −80 °C until Western blot analysis was performed. Another section was homogenised in 10 volumes of ice-cold physiological saline and spun at 15,000 rpm for 20 min at 4 °C. The supernatant was then stored at −80 °C for the ELISA of the levels of growth factors. Another section of each prostate was fixed in 4% paraformaldehyde for 3 days, embedded in paraffin, serially sectioned, and stained with haematoxylin–eosin. Immunohistochemical analysis was performed on deparaffinised sections. The sections were immersed in freshly prepared 3% H_2O_2 at 37 °C for 10 min and blocked with 5% goat serum for 10 min. Afterward, the sections were washed with PBS and incubated at 37 °C for 1 h with a primary antibody (anti-VEGF), treated with secondary antibody at 37 °C for 10 min, and immersed in diaminobenzidine for 3 min. The haematoxylin-stained sections were dehydrated with ethanol and visualised with an Olympus 1X71 optical microscope (Olympus, Japan).

2.4.3. The prostate index

The prostate index of each rat was the ratio of prostate weight to body weight (mg/g) (Babu, Veeresh, Patil, & Warke, 2010).

2.4.4. Assay for levels of PSA, DHT, epidermal growth factor (EGF), basic fibroblast growth factor (bFGF), and keratinocyte growth factor (KGF)

The assay for the levels of PSA, DHT, EGF, bFGF, and KGF was performed using specific ELISA kits (R&D Systems, Minneapolis, MN). All procedures were performed according to manufacturer's instructions. The results for PSA, DHT, EGF, bFGF, and KGF were expressed in pg/mL, nmol/L, pg/mL, pg/mL, and pg/mL, respectively.

2.4.5. Western blot analysis for Bax, Bcl-2, and p53

The expressions of Bax, Bcl-2, and p53 in the prostates were evaluated using Western blot analysis. Briefly, tissue samples were ground in liquid nitrogen, and protein concentrations were determined using a BCA protein assay kit (Pierce Biotechnology, Rockford, IL). Protein samples (50 μg) were separated through electrophoresis in 12% SDS–polyacrylamide gel, and then transferred onto PVDF membranes (Roche Diagnostics Corporation, Indianapolis, IN) via electrophoretic transfer (Bio-Rad Laboratories, Hercules, CA). Afterward, the membranes were blocked with 5% non-fat milk in Tris-buffered saline containing 0.1% Tween 20 (TBST) for 1 h at room temperature, and then incubated overnight at 4 °C with different primary antibodies (1:500 anti-Bax, anti-Bcl-2, and anti-p53). The membranes were then washed thrice with TBST, and then incubated with horseradish peroxidase-conjugated secondary antibodies (1:3000) in TBST with 3% non-fat milk for 1 h at room temperature. The immunoblots were developed on films using the enhanced chemiluminescence technique (Super Signal West Pico; Pierce Biotechnology, Rockford, IL). Data were normalised using β-actin (1:1000) as internal control.

2.4.6. Statistical analysis

The values were presented as means ± SD. Results were statistically analysed by performing one-way ANOVA followed by Tukey's multiple comparison test using SPSS 11.5 software for Windows (SPSS Inc., Chicago, IL). Differences were considered significant at $p < 0.05$.

3. Results

3.1. Chemical analysis

HPLC–DAD–MS/MS was used to analyse the flavonoid components of TFA and AHT. Fig. 1-II shows the results of HPLC of TFA and AHT. UV peaks and HPLC–MS data are listed in Table 1. The aglycone derivatives of flavan-4-ol glycoside, the main constituent of plants belonging to the genus *Abacopteris*, were identified by comparing the obtained UV characteristics and MS/MS fragmentation patterns of the compounds with data reported in previous phytochemical studies on *A. penangiana* (Wei, Wu, Lei, Xiong, & Ruan, 2011; Zhao et al., 2006; Zhao et al., 2007; Zhao et al., 2008; Zhao et al., 2010; Zhao et al., 2011). Up to 15 compounds, including 12 flavan-4-ol glycosides, were characterised. The presence of triphyllin A, eruberin B, abacopterin K, abacopterin I, 6″-*O*-acetyltriphyllin A, 6″-*O*-acetyleruberin B, 7-hydroxy-4′-methoxy-6,8-dimethylanthocyanidin, and 5,2′,5′-trihydroxy-7-methoxyflavanone in the tested samples was confirmed via co-injection of corresponding standard compounds.

Based on the total ion chromatogram (TIC) of TFA (Fig. 2), the typical *m/z* peaks of 297/299 were generally observed. These finding indicated the presence of the aglycone of 7-hydroxy-4′-methoxy-6,8-dimethylanthocyanidin, a desaccharified derivative of flavan-4-ol glycoside.

Peak 1 in the MS spectrum of TFA showed $[M+Na]^+$ at *m/z* 679, with MS^2 at *m/z* 477 $[M-Glc+H]^+$, *m/z* 459 $[M-Glc-H_2O+H]^+$, and *m/z* 297 $[M-2Glc+H]^+$, which are characteristic of triphyllin A (Zhao et al., 2006). With 42 mass units (acetyl group) more than triphyllin A, peak 5 showed $[M+Na]^+$ at *m/z* 721, with MS^2 at *m/z* 663 $[M-2H_2O+H]^+$, *m/z* 519 $[M-Glc+H]^+$, *m/z* 501 $[M-Glc-H_2O+H]^+$, and *m/z* 297 $[M-Glc-acetylGlc+H]^+$, which are diagnostic fragmentations of 6″-*O*-acetyltriphyllin A (Zhao et al., 2010). The identification of these peaks was confirmed via co-injection of corresponding standard compounds.

With 16 mass units less than triphyllin A, peak 2 showed $[M+Na]^+$ at *m/z* 663, with MS^2 at *m/z* 623 $[M-H_2O+H]^+$, *m/z* 461 $[M-Glc+H]^+$, and *m/z* 299 $[M-2Glc+H_2O+H]^+$. This fragmentation pattern perfectly reflects the structure of eruberin B (Zhao et al., 2007), which has one oxygen atom less than triphyllin A. Similar to peaks 1 and 5, peak 6 appeared at *m/z* 705, indicating that the compound it represents is an acetyl derivative of eruberin B. MS^2 was at *m/z* 503 $[M-Glc+H]^+$ and *m/z* 299 $[M-Glc-acetylGlc+H_2O+H]^+$; this fragmentation pattern is in accordance with the structure of 6″-*O*-acetyleruberin B (Zhao et al., 2008). The identification of these peaks was confirmed via co-injection of corresponding standard compounds.

Table 1
UV absorption, mass spectral data and putative identity of TFA components.

Compound	Rt (min)	UV wavelength (nm)	MS (*m/z*)	MS^2/MS^3 (*m/z*)	Putative identity
1	36.11	228 276	679	477 459 297	Triphyllin A
2	39.74 39.74	226 276	663	623 461 299	Eruberin B
3	48.18	228 277	643	459 297	Abacopterin K
4	50.53	226 278	645	461 299	Abacopterin I
5	51.82	226 279	721	663 519 501 297	6″-*O*-Acetyltriphyllin A
6	52.56	225 279	705	503 299	6″-*O*-Acetyleruberin B
7	57.81	227 275	687	503 299	Acetylabacopterin I
8	59.43	280 325	501	297	7-Hydroxy-4′-methoxy-6,8-dimethylanthocyanidin acetyl glucopyranoside
9[a]	64.67	278 330	297	297	7-Hydroxy-4′-methoxy-6,8-dimethylanthocyanidin
10[b]	65.11	232 280	461 943	299	Abacopterin C/Eruberin A
11	68.04	220 290	303	167	5,2′,5′-Trihydroxy-7-methoxyflavanone
12[b]	69.20	230 280	461 943	299	Abacopterin C/Eruberin A
13[b]	75.01	227 275	503	299	Abacopterin A/Abacopterin B/6″-*O*-Acetyleruberin A
14[b]	78.56	225 279	503	299	Abacopterin A/Abacopterin B/6″-*O*-Acetyleruberin A
15[b]	79.57	228 280	503	297	Abacopterin A/Abacopterin B/6″-*O*-Acetyleruberin A

[a] The HPLC–MS/MS analysis of AHT resulted in the same data (Rt, MS, MS^2/MS^3) as compound 9.
[b] These compounds are isomers.

Peak 3 showed $[M+Na]^+$ at *m/z* 643, with MS^2 at *m/z* 459 $[M-Glc+H_2O+H]^+$ and *m/z* 297 $[M-2Glc+2H_2O+H]^+$. Peak 4 showed $[M+Na]^+$ at *m/z* 645, with MS^2 at *m/z* 461 $[M-Glc+H_2O+H]^+$ and *m/z* 299 $[M-2Glc+2H_2O+H]^+$. These patterns reflect abacopterin K (Zhao et al., 2011) and abacopterin I (Zhao et al., 2007), identified via co-injection of corresponding standard compounds. Having 42 mass units (the acetyl group) more than abacopterin I, peak 7 showed $[M+Na]^+$ at *m/z* 687, with MS^2 at *m/z* 503 $[M-Glc+H_2O+H]^+$ and *m/z* 299 $[M-Glc-acetylGlc+H_2O+H]^+$. With this pattern, the acetyl derivative of abacopterin I was tentatively identified, but the presence of acetyl in the glucose could not be determined.

Peak 9 showed $[M+H]^+$ at *m/z* 297 and peak 11 showed $[M+H]^+$ at *m/z* 303, which were identified as 7-hydroxy-4′-methoxy-6,8-dimethylanthocyanidin (Zhao et al., 2006) and 5,2′,5′-trihydroxy-7-methoxyflavanone (Wei et al., 2011), respectively, via co-injection of corresponding standard compounds. Peak 8 showed $[M+H]^+$ at *m/z* 501, with MS^2 at *m/z* 297. Its loss of 204 mass units indicated that it represents an acetyl glucose (–acetylGlc + H_2O). Hence, peak 8 was putatively identified as 7-hydroxy-4′-methoxy-6,8-dimethylanthocyanidin acetyl glucopyranoside. The attachment site and the presence of acetyl in the glucose could not be determined.

Previous studies have suggested that some isomers exist in *A. penangiana*. In the present investigation, peaks 10 and 12 showed the same MS peak at *m/z* 461 $[M+H]^+$ and *m/z* 943 $[2\,M+Na]^+$ and the same MS^2 peak at *m/z* 299. These data were in accordance with the structures of abacopterin C (Zhao et al., 2006) and eruberin A (Zhao et al., 2007), respectively, which were previously isolated from *A. penangiana*. The only difference in the structures of these compounds is the spatial configuration at C-4. Similarly, peaks 13, 14, and 15 showed the same molecular ion peak at *m/z* 503 $[M+H]^+$ (Fig. 2) and the same MS^2 peak at *m/z* 299/297. The compounds these peaks represent were tentatively identified as abacopterin A, abacopterin B, and 6″-*O*-acetyleruberin A (Zhao et al., 2006), respectively, which are isomers with different configurations at C-4 or different acetyl positions in the glucose.

Furthermore, the examination of the UV spectra of the samples supported the above identifications. Peaks 1–7, 10, and 12–15 showed very similar UV spectra, with absorption peaks at around 228 and 276 nm. These data are characteristic of flavan-4-ol glycosides.

HPLC of AHT showed only one main peak, which had the same retention time and mass characteristics as that of 7-hydroxy-4′-methoxy-6,8-dimethylanthocyanidin in TFA. This identification was confirmed via co-injection with a corresponding standard compound. Results indicated that 7-hydroxy-4′-methoxy-6,8-dimethylanthocyanidin is the main product of the acid hydrolysis of TFA. The said compound belongs to 3-deoxygenated anthocyanidins, which are rarely found in nature.

3.2. Histological and immunohistochemical analysis

The effects of TFA and AHT on prostate gland morphology are shown in Fig. 3. There was no change in the histoarchitecture of the prostate gland of rats in the negative control group; tissues were tightly packed and epithelium cells were cuboidal and regular in size (Fig. 3A). The glands of rats in the BPH model group (Fig. 3B) showed typical patterns of glandular hyperplasia: papillary fronds in epithelial cells with vacuolated (multiple vacuoles) cytoplasm projecting into the glandular lumen, and decreased glandular luminal area. After 4 weeks of administering finasteride, TFA, and AHT, a marked increase in the luminal volume was observed (Fig. 3C–G). The glandular epithelial height of the groups given these treatments was significantly reduced compared with that of the BPH model group.

The expression of VEGF in the rat prostates was examined through immunohistochemical analysis. As shown in Fig. 3, VEGF was rarely expressed in normal prostatic glandular epithelial cells. A significant increase in VEGF expression was detected in the prostatic glandular epithelial cells of the BPH model group. Conversely, the expression was reduced in the rats administered with TFA and AHT, especially those given a dose of 200 mg/kg per day.

3.3. Prostate index changes

Prostate index is commonly used to evaluate the development of BPH. Compared with rats in the negative control group, those injected with testosterone had significantly higher prostate indices (Table 2), suggesting that testosterone successfully induced BPH in the castrated rats. Compared with rats in the BPH model group however, testosterone-treated rats given TFA (200 mg/kg per day, $P < 0.05$) and AHT (200 mg/kg per day, $P < 0.01$) had remarkably lower prostate indices. This result indicated that TFA and AHT have potential for treatment of BPH.

3.4. ELISA for PSA, DHT, EGF, bFGF, and KGF

The levels of PSA, DHT, and prostatic growth factors EGF, bFGF, and KGF were determined via ELISA. Data in Table 2 indicate that the prostates of rats in the BPH model group had increased levels of PSA, DHT, and growth factors (all three). PSA is a biomarker that indicates the occurrence of BPH and prostate cancer. In this study,

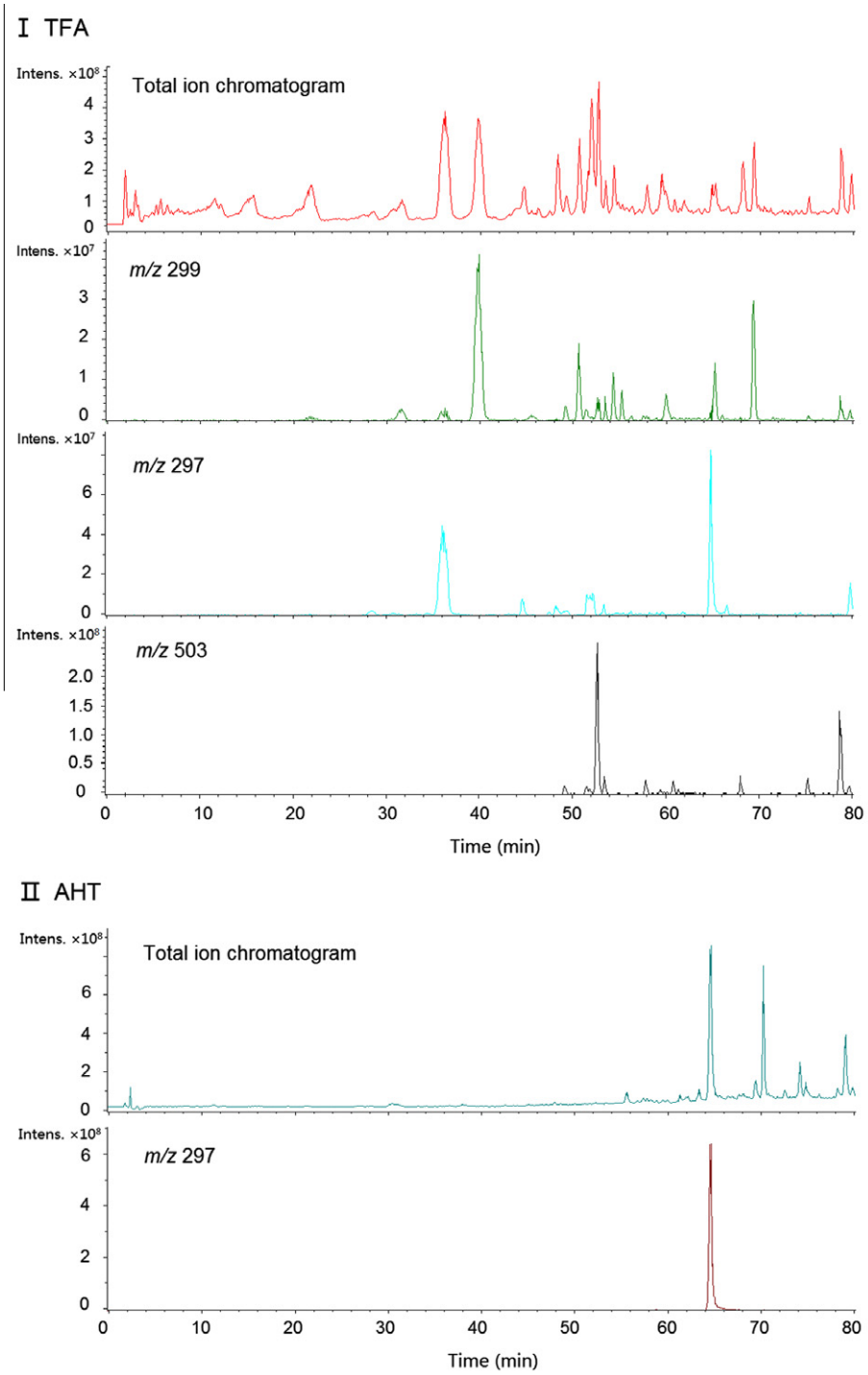

Fig. 2. Total ion chromatogram and selective ion chromatograms of TFA (I) and AHT (II).

daily administration of TFA and AHT for 4 weeks decreased the serum PSA and DHT levels. In addition, long-term administration of TFA and AHT reduced prostatic levels of EGF, bFGF, and KGF, which were considered to play key roles in BPH.

3.5. Western blot analysis for Bax, Bcl-2, and p53

The disruption of apoptotic equilibrium is an important factor in the pathogenesis of BPH. Western blot analysis was performed to investigate the effects of TFA and AHT on prostatic cell apoptosis. As shown in Fig. 4, the expression of Bcl-2 was markedly upregulated in the prostates of rats in the BPH model group, compared with rats in the negative control group. In addition, the expressions of Bax and p53 in the prostates of rats treated with TFA and AHT were significantly increased, compared with rats in the BPH model group, indicating that TFA and AHT enhance cell apoptosis in hyperplastic prostates.

4. Discussion

In this study, the chemical constituents of TFA and AHT were first determined via HPLC–DAD–ESI–MS/MS analysis. Results

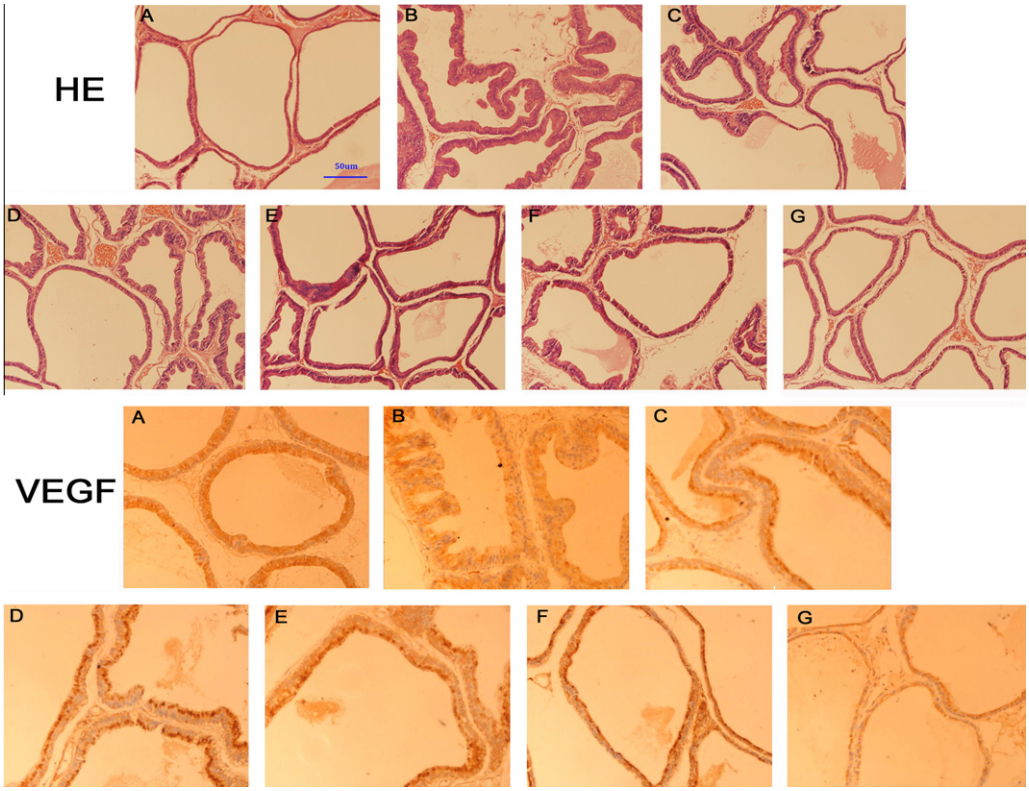

Fig. 3. Histological and immunohistochemical findings from prostate sections in the rat model of BPH. (A) Negative control group; (B) BPH model group; (C) positive control group; (D) TFA (100 mg/kg per day) treated group; (E) TFA (200 mg/kg per day) treated group; (F) AHT (100 mg/kg per day) treated group; (G) AHT (200 mg/kg per day) treated group. HE, haematoxylin eosin; VEGF, vascular endothelial growth factor.

Table 2
Results of prostatic index changes and ELISA.

Groups	Prostate index (mg/g)	ELISA				
		PSA (pg/mL)	DHT (nmol/L)	EGF (pg/mL)	bFGF (pg/mL)	KGF (pg/mL)
I	3.09 ± 0.15	158 ± 16.01	3.11 ± 0.11	61.2 ± 4.73	2.83 ± 0.10	98.6 ± 10.5
II	5.53 ± 0.20[a]	336 ± 6.44[a]	5.34 ± 0.49[b]	203 ± 2.02[a]	6.29 ± 0.05[a]	210 ± 16.5[a]
III	4.82 ± 0.16[c]	202 ± 19.2[d]	2.08 ± 0.10[d]	72.1 ± 2.39[d]	2.81 ± 0.38[d]	93.0 ± 9.89[d]
IV	5.15 ± 0.15	198 ± 28.4[c]	2.88 ± 0.14[d]	115 ± 11.62[d]	3.48 ± 0.16[d]	99.3 ± 6.44[d]
V	4.90 ± 0.18[c]	183 ± 15.5[d]	2.47 ± 0.12[d]	74.0 ± 4.90[d]	3.07 ± 0.25[d]	93.4 ± 10.4[d]
VI	5.03 ± 0.22	189 ± 33.4[c]	3.32 ± 0.20[c]	90.7 ± 11.02[d]	3.18 ± 0.29[d]	100 ± 2.73[d]
VII	4.44 ± 0.22[d]	160 ± 21.7[d]	2.56 ± 0.17[d]	73.6 ± 1.60[d]	2.97 ± 0.27[d]	77.7 ± 1.96[d]

Data were presented as means ± SD of six rats. *Group I:* negative control group; *Group II:* BPH model group; *Group III:* positive control group; *Group IV:* TFA (100 mg/kg per day) treated group; *Group V:* TFA (200 mg/kg per day) treated group; *Group VI:* AHT (100 mg/kg per day) treated group; *Group VII:* AHT (200 mg/kg per day) treated group. PSA, prostate-specific antigen; DHT, dihydrotestosterone; EGF, epidermal growth factor; bFGF, basic fibroblast growth factor; KGF, keratinocyte growth factor.

[a] $P < 0.01$.

[b] $P < 0.05$ versus negative control rats.

[c] $P < 0.05$.

[d] $P < 0.01$ versus model rats.

indicate that TFA mainly contains flavan-4-ol glycosides, whereas the main constituent of AHT is 7-hydroxy-4′-methoxy-6,8-dimethylanthocyanidin, a desaccharified derivative of flavan-4-ol glycosides. Afterwards, the anti-BPH potential of TFA and AHT in rats with testosterone-induced prostatic hyperplasia was evaluated. Results showed that the administration of TFA or AHT for 4 weeks significantly inhibits the development of testosterone-induced prostatic hyperplasia, as proven by the reduction in prostatic indices and PSA levels, as well as histopathological findings.

BPH is a multifactorial disease and the most common non-cancerous abnormal prostate cell growth. Hormonal changes and enhanced proliferation and suppression of apoptosis of prostatic cells are believed to play important roles in BPH (Briganti et al., 2009; Liu et al., 2007; Novara, Galfano, Berto, Ficarra, Navarrete, & Artiban, 2006). In this study, the effects of TFA/AHT on these three factors were investigated.

Testosterone and other related hormones have been demonstrated to be involved in BPH. The main prostatic androgen is DHT, which is formed by the steroid enzyme 5α-reductase from testosterone. The production and accumulation of DHT in the prostate encourage cell growth and induce hyperplasia (Sun et al., 2008). This investigation was performed in BPH rat models generated by subcutaneous injection of testosterone after castration. The increased prostatic indices of the rat models confirmed the influence of androgens on BPH. Decreased serum DHT levels in TFA/AHT-treated rats indicated that TFA and AHT inhibit the activity of 5α-reductase. Finasteride (positive control) was used to inhibit BPH by serving as an enzyme blocker against 5α-reductase.

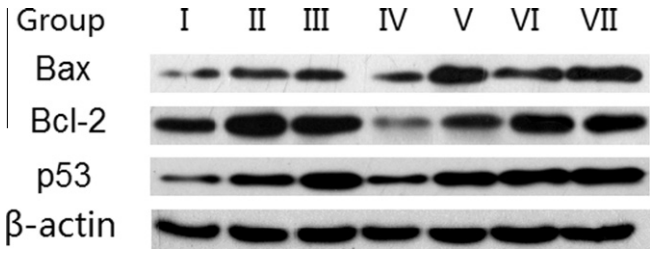

Fig. 4. Effects of TFA and AHT on the expression of Bax, Bcl-2 and p53. *Group I:* negative control group; *Group II:* BPH model group; *Group III:* positive control group; *Group IV:* TFA (100 mg/kg per day) treated group; *Group V:* TFA (200 mg/kg per day) treated group; *Group VI:* AHT (100 mg/kg per day) treated group; *Group VII:* AHT (200 mg/kg per day) treated group.

Increasing evidence suggests that androgens have a permissive role in the growth of prostate (Ilio, Sensibar, & Lee, 1995). By contrast, other evidence also suggests that prostate growth is under the indirect control of androgens through the mediation of different growth factors (Levine et al., 1998).

There is a possibility that fibroblast growth factors (FGFs) play an important role in prostate growth because they exhibit mitogen and angiogenic activities. The main FGFs in the prostate are KGF and bFGF (Ittmann & Mansukhani, 1997). The concentrations of bFGF and KGF have been proven to be increased in hyperplastic tissues compared with levels in normal prostate tissues (Boget, Leriche, & Rovel, 2001). This finding was confirmed in this study by the greatly elevated levels of bFGF and KGF in the prostates of BPH rat models observed. The reduced concentration of bFGF and KGF in the TFA/AHT-treated rats suggests that TFA and AHT exert anti-BPH effects by decreasing the levels of prostatic growth factors. DHT has been reported to increase the transcription of VEGF and the secretion of biologically active VEGF from human prostatic stroma (Sun et al., 2008). VEGF is a major inducer of angiogenesis as it influences endothelial cell growth (Neufeld, Cohen, Gengrinovitch, & Poltorak, 1999). EGF, a mitogen of rat prostatic epithelial cells (*in vivo* and *in vitro*), has been proven to greatly enhance the expression of VEGF in BPH (Ravindranath, Wion, Brachet, & Djakiewe, 2001). Hence, the attenuated VEGF expression in the prostatic gland epidermal cells of TFA/AHT-treated rats observed in this study may have been due to the reduced levels of EGF.

BPH is a slow progressive disease characterised by the abnormal enlargement of prostate glands, leading to heterogeneous gland morphology. The disruption of apoptotic pathways has been suggested to be an important regulatory mechanism in this common disease, which has significant morbidity. This mechanism leads to the pathological accumulation of cells and perpetuation of abnormal gene expression (Gandour-Edwards, Mack, deVere-White, & Gumerlock, 2004). Some of the major regulatory apoptotic proteins that have been identified are the anti-apoptotic factor Bcl-2, and the pro-apoptotic factors Bax and p53. The p53 tumour suppressor gene plays an important role in the control of the cell cycle (Schlechtea et al., 1998). In addition, Bax and Bcl-2 are noted to form homo- and heterodimers, and the ratio of their dimeric forms determine whether cells would continue to survive or undergo apoptosis (Basu & Haldar, 1998). In the prostates of the BPH rat models, Bcl-2 expression was markedly upregulated compared with rats in the negative control group. The overexpression of Bcl-2 reduced apoptosis and eventually resulted in BPH. Moreover, the expressions of Bax and p53 in the prostates of TFA/AHT-treated rats were significantly increased compared with BPH rat models, indicating that TFA/AHT administration enhances apoptosis, leading to the attenuation of BPH.

In summary, TFA and AHT exert anti-BPH effects via three major mechanisms. First, TFA and AHT reduce serum DHT concentrations by inhibiting the activity of 5α-reductase enzyme. Second, TFA and AHT ameliorate BPH by decreasing the levels of prostatic VEGF, EGF, bFGF, and KGF. Lastly, TFA and AHT attenuate the disruption of apoptosis, which occurs in BPH. Generally, the anti-BPH effect of AHT is stronger than that of TFA (administered at the same dose). Further work should be conducted to determine the anti-BPH potential of flavan-4-ol glycosides and 7-hydroxy-4′-methoxy-6,8-dimethylanthocyanidin, which are the main constituents of TFA and AHT, respectively.

Acknowledgement

This work was supported by the National Natural Science Foundation of China (No.: 81173065).

References

Babu, S. V. V., Veeresh, B., Patil, A. A., & Warke, Y. B. (2010). Lauric acid and myristic acid prevent testosterone induced prostatic hyperplasia in rats. *European Journal of Pharmacology, 626*, 262–265.

Basu, A., & Haldar, S. (1998). The relationship between BCL2, BAX and p53: consequences for cell cycle progression and cell death. *Molecular Human Reproduction, 4*, 1089–1109.

Boget, S., Leriche, A., & Rovel, A. (2001). Basic fibroblast growth factor and keratinocyte growth factor over-expression in benign prostatic hyperplasia. *Il Farmaco, 56*, 467–469.

Briganti, A., Capitanio, U., Suardi, N., Gallina, A., Salonia, A., Bianchi, M., et al. (2009). Benign prostatic hyperplasia and its aetiologies. *European Urology Supplements, 8*, 865–871.

Chen, J., Chen, X., Lei, Y., Wei, H., Xiong, C., Liu, Y., et al. (2011). Vascular protective potential of the total flavanol glycosides from *Abacopteris penangiana* via modulating nuclear transcription factor-κB signaling pathway and oxidative stress. *Journal of Ethnopharmacology, 136*, 217–223.

Gandour-Edwards, R., Mack, P. C., deVere-White, R. W., & Gumerlock, P. H. (2004). Abnormalities of apoptotic and cell cycle regulatory proteins in distinct histopathologic components of benign prostatic hyperplasia. *Prostate Cancer and Prostatic Disease, 7*, 321–326.

Ilio, K. Y., Sensibar, J. A., & Lee, C. (1995). Effect of TGF-α, TGF-β, and EGF on cell proliferation and cell death in rat ventral prostatic epithelial cells in culture. *Journal of Andrology, 16*, 482–490.

Ittmann, M., & Mansukhani, A. (1997). Expression of fibroblast growth factors (FGFs) and FGF receptors in human prostate. *Journal of Urology, 157*, 351–356.

Jang, H., Ha, U. S., Kim, S. J., Yoon, B. I., Han, D. S., Yuk, S. M., et al. (2010). Anthocyanin extracted from black soybean reduces prostate weight and promotes apoptosis in the prostatic hyperplasia-induced rat model. *Journal of Agricultural and Food Chemistry, 58*, 12686–12691.

Levine, A. C., Liu, X. H., Greenberg, P. D., Eliashvili, M., Schiff, J. D., Aaronson, S. A., et al. (1998). Androgens induce the expression of vascular endothelial growth factor in human fetal prostatic fibroblasts. *Endocrinology, 139*, 4672–4678.

Liu, C., Huang, S., Li, W., Wang, C., Chou, Y., Li, C., et al. (2007). Relationship between serum testosterone and measures of benign prostatic hyperplasia in aging men. *Urology, 70*, 677–680.

Nahata, A., & Dixit, V. K. (2011). *Sphaeranthus indicus* attenuates testosterone induced prostatic hypertrophy in albino rats. *Phytotherapy Research, 25*, 1839–1848.

Napalkov, P., Maisonneuve, P., & Boyle, P. (1995). Worldwide patterns of prevalence and mortality from benign prostatic hyperplasia. *Urology, 46*, 41–46.

Naslund, M. J., & Coffey, D. S. (1986). The differential effects of neonatal androgens, estrogen and progesterone on adult rat prostate growth. *Journal of Urology, 136*, 1136–1140.

Neufeld, G., Cohen, T., Gengrinovitch, S., & Poltorak, Z. (1999). Vascular endothelial growth factor (VEGF) and its receptors. *The FASEB Journal, 13*, 9–22.

Novara, G., Galfano, A., Berto, R. B., Ficarra, V., Navarrete, R. V., & Artiban, W. (2006). Inflammation, apoptosis, and BPH: What is the evidence? *European Urology Supplements, 5*, 401–409.

Pérez, Y., Molina, V., Mas, R., Menéndez, R., González, R. M., Oyarzábal, A., et al. (2008). *Ex vivo* antioxidant effects of D-004, a lipid extract from *Roystonea regia* fruits, on rat prostate tissue. *Asian Journal of Andrology, 10*, 659–666.

Ravindranath, N., Wion, D., Brachet, P., & Djakiewe, D. (2001). Epidermal growth factor modulates the expression of vascular endothelial growth factor in the human prostate. *Journal of Andrology, 22*, 432–443.

Schlechtea, H., Lenka, S. V., Löning, T., Schnorr, D., Rudolph, B., Ditscherlein, G., et al. (1998). P53 Tumour suppressor gene mutations in benign prostatic hyperplasia and prostate cancer. *European Urology, 34*, 433–440.

Skaudickas, D., Kondrotas, A. J., Kevelaitis, E., & Venskutonis, P. R. (2009). The effect of *Echinacea purpurea* (L.) Moench extract on experimental prostate hyperplasia. *Phytotherapy Reseasrch, 23*, 1474–1478.

Sun, H., Li, T., Sun, L., Qiu, Y., Huang, B., Yi, B., et al. (2008). Inhibitory effect of traditional Chinese medicine Zi-Shen Pill on benign prostatic hyperplasia in rats. *Journal of ethnopharmacology, 115*, 203–208.

Thompson, T. C., & Yang, G. (2009). Regulation of apoptosis in prostatic disease. *Prostate Supplements, 9*, 25–28.

Untergasser, G., Madersbacher, S., & Berger, P. (2005). Benign prostatic hyperplasia: age-related tissue-remodeling. *Experiemtal Gerontology, 40*, 121–128.

Wei, H., Wu, G., Lei, Y., Xiong, C., & Ruan, J. (2011). Neuropective constituents from the rhizomes of *Abacopteris penangiana*. *Journal of Asian Natural Products Research, 13*, 707–713.

Wei, H., Ruan, J., Lei, Y., & Yang, C. (2012). Enrichment and purification of flavones from rhizomes of *Abacopteris penangiana* by macroporous resins. *Chinese Journal of Natural Medicines, 10*, 119–124.

Zhao, Z., Ruan, J., Jin, J., Zou, J., Zhou, D., Fang, W., et al. (2006). Flavan-4-ol glycosides from the rhizomes of *Abacopteris penangiana*. *Journal of Natural Products, 69*, 265–268.

Zhao, Z., Jin, J., Ruan, J., Zhu, C., Lin, C., Fang, W., et al. (2007). Antioxidant flavonoid glycosides from aerial parts of the fern *Abacopteris penangiana*. *Journal of Natural Products, 70*, 1683–1686.

Zhao, Z., Jin, J., Ruan, J., Cai, Y., & Zhu, C. (2008). Two new flavan glycosides from *Abacopteris penangiana*. *Acta pharmaceutica Sinica, 43*, 392–395.

Zhao, Z., Ruan, J., Jin, J., Zhu, C., & Lin, C. (2010). Two new acetylated flavan glycosides from rhizomes of the fern *Abacopteris penangiana*. *Journal of Asian Natural Products Research, 12*, 1015–1019.

Zhao, Z., Ruan, J., Jin, J., Zhu, C., & Yu, Y. (2011). Two new flavonoids from the rhizomes of *Abacopteris penangiana*. *Helvetica Chimica Acta, 94*, 446–452.